Journal of Biomechanical Science and Engineering

Vol. 5, No. 1, 2010

Simulation of Force Changes in the Human Biceps Using a Muscle Model Based on Electromyographic Signals*

Akira ITO**, Masami SAITO** and Youjiro TAMURA***

**Department of Electronic and Information Engineering, Suzuka National College of Technology, Suzuka, Mie 510-0294, Japan

E-mail: aito@info.suzuka-ct.ac.jp

***Department of Physics, Suzuka National College of Technology, Suzuka, Mie 510-0294, Japan

Abstract

The purpose of this study was to reproduce the force in a voluntary contraction via surface electromyography (SEMG) using a systematic muscle model. We measured the isometric voluntary contractile force and SEMG of the human biceps. We examined the effect of the electrode size on SEMG. A pair of electrodes with a diameter of 1 mm was adopted, because they avoided signal interference from the action potentials of other motor units. We added a converter to the muscle model to obtain an artificial action potential that successively drives an excitation-contraction controller and a motor unit. When the force was less than 30% of the maximum force, EMG signals were obtained from a few motor units. The resultant force coincided well with the experimentally observed force with an accuracy of around 90% when an appropriate threshold level was set up in the converter. This method will increase in performance when we can separately detect the SEMG signals from multipoint measurements.

Key words: Muscle, Model, Electromyography, Numerical Simulation, Excitation-Contraction Coupling

1. Introduction

Skeletal muscle comprises several hundred motor units. Each motor unit is a functional unit that produces force and consists of a motor neuron and muscle fibers[1]. Therefore, many investigators have measured electromyography (EMG) signals to study the functions of motor neurons and analyzed force changes to study the mechanical properties of muscle fibers[1-7]. EMG measurements are obtained with two types of electrodes, namely indwelling and surface electrodes[2]. Although a needle electrode can catch an action potential from a single motor unit, not all investigators are legally allowed to insert a needle electrode into the human body. On the other hand, surface EMG (SEMG) is popular because the measurement technique is noninvasive. However, SEMG is disturbed by the signals from several motor units, depending on the size and distance of the electrodes[3].

In this study, we investigated whether smaller surface electrodes are suitable for recording SEMG signals. We used surface electrodes with a diameter of 1 mm to avoid interference from the action potentials of other motor neurons as much as possible. We newly added a converter to a systematic muscle model that we described in previous reports[8-10]. The model overcomes many limitations of Hill-type models[11-13]. The converter outputs an artificial action potential (AAP) from the SEMG signal and the AAP is put into an excitation-contraction (E-C) controller of the muscle model. We demonstrated that our

*Received 1 July, 2009 (No. 09-0298)
[DOI: 10.1299/jbse.5.18]

muscle model was able to reproduce the voluntary contractile force from SEMG signals. We then evaluated the accuracy of the resultant force by reference to the force obtained experimentally.

2. Experimental Methods

2.1. Measurements

Three clinically healthy male subjects participated in this experiment. The subjects ranged in age from 19–22 years and provided informed consent. The force exerted by the human biceps was recorded using the apparatus shown in Fig. 1(a). Each subject was seated in a chair and their upper arm was placed and stabilized on the arm-bed. The elbow was flexed perpendicular to the horizontal plane to avoid a gravity effect of the forearm. The forearm was always set in contact with a stick at a position just below the wrist, and the palm of the hand was kept flat so that no muscle groups other than the biceps brachii were activated. The force was measured by transducers attached to the stick as shown in Fig. 1(b). When the angle θ was kept constant in an isometric contraction, the force of the biceps brachii was proportional to the measured force. The force was controlled within 30% of the isometric maximum voluntary contraction (MVC) to avoid interference between the action potentials and fatigue.

The skin above the investigated muscles was cleaned with an alcohol wipe. We created three pairs of test electrodes (10 mm × 10 mm, 10 mm × 2 mm and 1 mm × 1 mm), as shown in Fig. 1(c), to confirm the effect of the electrode size on SEMG. The electrodes were made from Cu by a wet etching process. The electrodes faced each other with a gap of 10 mm and were oriented along the muscle fibers. The electrodes were positioned along the middle of the muscle belly on the biceps brachii. When the electrodes were re-attached, we placed each electrode carefully to maintain the signal peak maximum, because SEMG signals are sensitively dependent on the electrode position. Finally, a pair of Ag electrodes with a diameter of 1 mm was made to measure the SEMG signals because Ag does not rust. The SEMG signals were amplified using an oscilloscope (VC-11; Nihon Kohden) with a

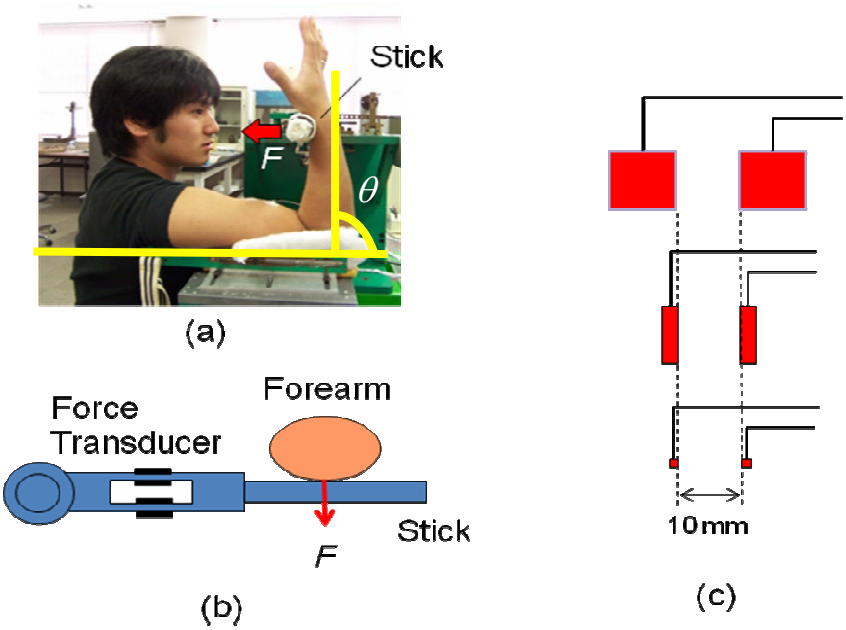

Fig. 1 Experimental apparatus and set-up. (a) The position and posture of each subject against the apparatus. (b) Top view of the force measurement stick and transducer. (c) Three pairs of test electrodes (10 mm × 10 mm, 10 mm × 2 mm and 1 mm × 1 mm) were created to confirm the effect of the electrode size on SEMG.

band-pass filter (50–10000 Hz). Force and SEMG signals were simultaneously recorded on a personal computer through a 16-bit A/D converter (WE7271; Yokogawa) with a sampling frequency of 10 kHz.

2.2. Numerical Calculations

Numerical calculations were carried out using a biceps-forearm system model. Figure 2(a) shows a block diagram of the converter, E-C controller and muscle model. The converter changes the SEMG signals into an AAP. In the converter, AAP pulse trains are obtained at the peak of the SEMG signals when they are above a certain threshold level. We set the duration of the AAP to 1 ms, by reference to the action potential of fast twitch muscle[6]. The AAP pulse trains drive the E-C controller. The E-C controller is based on the chemical scheme of myosin cross-bridges and outputs the weights Nd_1 and Nd_2 to regulate the force of the muscle model[8-10]. Figure 2(b) shows the geometry of the muscle model for the human biceps and forearm. The muscle model consists of two parallel Maxwell elements, one Voight element and a force generator. The spring constants are shown by k, the viscosity components by C and the force generator by P (=1 or 0). The force of the muscle model (CAL-FORCE) is calculated by solving the equations of motions using the Runge-Kutta method. The CAL-FORCE is fed back to the E-C controller. This loop provides the muscle model with the complexity and nonlinearity of skeletal muscle. The muscle model can produce fast twitch and slow twitch skeletal muscle contractions by changing the chemical parameters in the E-C controller[10]. The human biceps is composed of almost equal amounts of slow twitch and fast twitch muscles[14,15]. However, we assumed that the contractile force of the biceps is dominated by fast twitch muscle under our experimental conditions, and adopted fast twitch muscle for the muscle model in this simulation[10]. The resultant force was calculated by smoothing of the CAL-FORCE with a window size of 0.5 s. The CAL-FORCE and smoothed CAL-FORCE were compared with the experimentally obtained force.

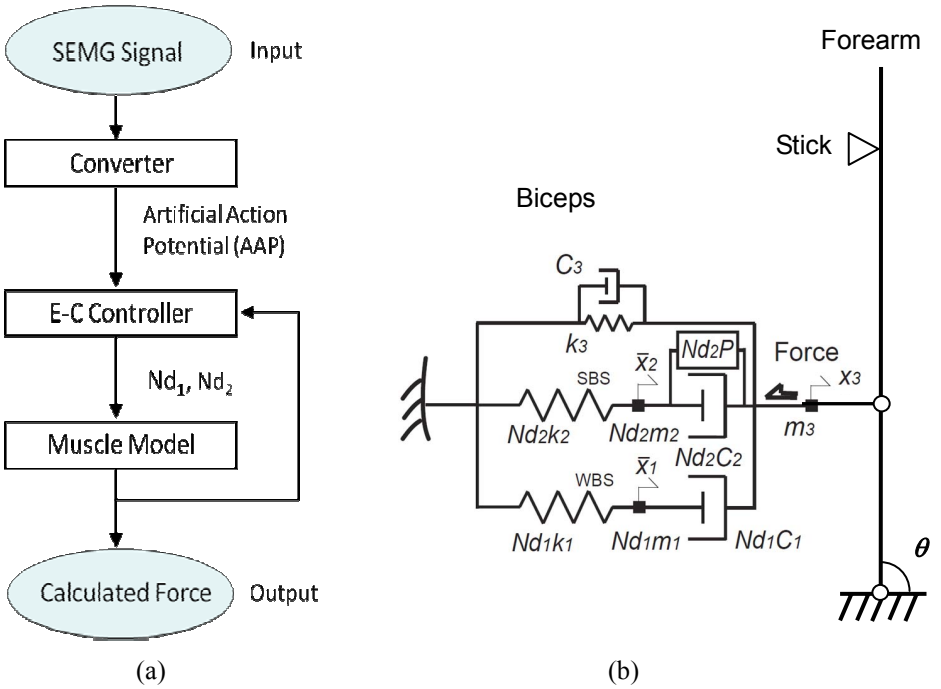

Fig. 2 Biceps-forearm system model. (a) Block diagram of the converter, E-C controller and muscle model. (b) Geometry of the muscle model for the human biceps and forearm.

3. Results and Discussion

Figure 3 shows representative SEMG signals for one subject for the three different sizes of electrodes, when the electrodes were placed in almost the same positions on the biceps brachii. In the case of the larger electrodes shown in Fig. 3 (a) and (b), the SEMG signals overlapped with each other among the many action potentials, even when the force was 10% of the MVC. On the other hand, in the case of the smallest electrodes shown in Fig. 3(c), the SEMG signals showed a spike-like pulse train under the same force condition. This pulse train comprised the action potentials from a few muscle fibers. The independence of the pulse was caused by the small size of the electrodes, which decreased the number and width of the signals from the muscle fibers. We found that the small electrodes were suitable for obtaining pulses independently below 30% of the MVC by changing the force conditions. Thereafter, we used a pair of Ag electrodes with a diameter of 1 mm.

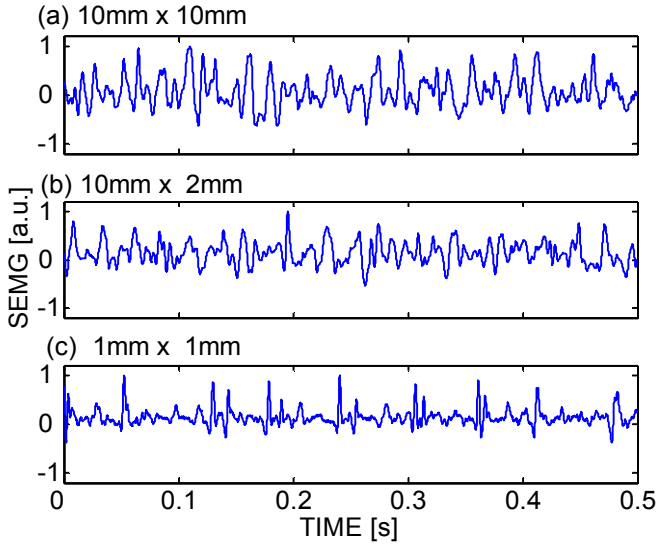

Fig. 3 Representative SEMG signals for one subject for the three different sizes of electrodes. (a) 10 mm × 10 mm. (b) 10 mm × 2 mm. (c) 1 mm × 1 mm.

Figure 4 shows typical results for the experimentally observed force (FORCE), SEMG, AAP, AAP frequency (f) and calculated force (CAL-FORCE) of two contraction patterns in case (1) and case (2). The two contraction patterns were successively carried out on one subject before the electrodes were removed. The small electrodes detected the SEMG signals, of which the pulse amplitude hardly changed and the pulse density varied with the force as shown in the EMG data in Fig. 4. The CAL-FORCE and smoothed CAL-FORCE data were plotted with a solid blue line and a dashed red line, respectively. The values were normalized by their maximum values. In case (1), the FORCE maintained middle, high and middle level forces with time, while in case (2), the FORCE maintained high, middle and high plateaus. The AAP pulse trains in case (1) and case (2) were calculated through the same threshold value of SEMG in the converter. When the force level was high, the APP pulse density increased, but the pulse amplitude hardly changed. The APP frequency was obtained from the reciprocal of the interpulse time of the AAP. The APP frequency also increased with the FORCE. It has been reported that the mean firing rate (±SD) of a biceps brachii muscle is 31.1±10.1 Hz during MVC based on needle EMG measurements[7]. Although the high frequency above 30 Hz was caused by interference from the action potentials of other motor units, most of the action potentials were obtained separately in our experiment. The APP frequencies were scattered more significantly above 30% of the MVC than below 30% of the MVC. As the force increased, the SEMG peak height increased with signal overlapping. Although the SEMG signals even overlapped at 10% of the MVC with

the large electrodes as shown in Fig. 3 (a) and (b), the small electrodes expanded the applicable force range to 30% of the MVC.

The CAL-FORCE almost coincided with the experimentally observed force. The CAL-FORCE exhibited oscillations, which were ascribed to the twitch force of fast twitch muscle. The force estimation error was quantified using the root mean square values as follows:

$$Error = \sqrt{\frac{\sum_{i=1}^{N}\left(FORCE(t_i) - CALFORCE(t_i)\right)^2}{N}}$$

where N is the sampling data point number. The errors in the CAL-FORCE were about 15% and 12% for case (1) and case (2) in Fig. 4, respectively. The errors in the smoothed CAL-FORCE were 12% and 9%, respectively. For the other two subjects, the errors in the smoothed CAL-FORCE were 12% and 13% for case (1), and 14% and 12% for case (2). No significant differences were observed among the subjects. If we can obtain AAP pulse trains from several motor units, the accuracy of the CAL-FORCE will improve. We are preparing experiments to simulate multi-motor unit contraction responses from SEMG data measured by multi-electrodes.

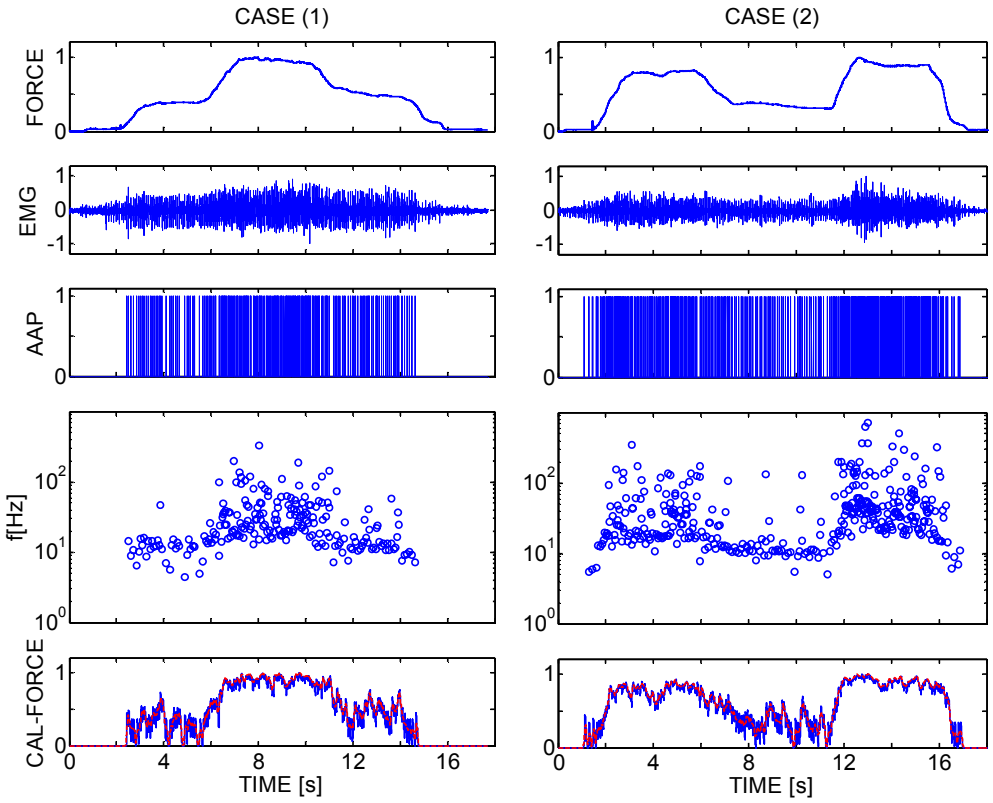

Fig. 4 Representative time courses of the measured force (FORCE), SEMG, artificial action potential (AAP), AAP frequency (f) and calculated force (CAL-FORCE) of two contraction patterns for one subject. The smoothed CAL-FORCE is also shown by a dashed red line.

4. Conclusions

We successfully detected SEMG signals from a few motor units using electrodes with a diameter of 1 mm. These electrodes enabled us to reproduce the force when the contractile force was less than 30% of the MVC. If we can detect SEMG signals separately by changing the configuration of the electrodes, this method will increase in performance for simulation of the kinetic behavior of the human musculoskeletal system for medical and engineering purposes.

References

(1) Enoka, M. R., *Neuromechanics of Human Movement,* (2008), Human Kinetics
(2) Merletti, R., and Parker, P. A. ed., *Electromyography. Physiology, Engineering, and Noninvasive Applications,* (2004), Wiley-Interscience
(3) Keenan, G. K., Farina, D., Maluf, S. K., Merletti, R. and Enoka, M. R., Influence of amplitude cancellation on the simulated surface electromyogram, *Journal of Applied Physiology*, Vol. 98 (2005), pp.120-131
(4) Liu, M. M., Herzog, W., and Savelberg, H. H.C.M., Dynamic muscle force predictions from EMG: an artificial neural network approach, *Journal of Electromyography Kinesiology*, Vol.9 (1999) pp.391-400
(5) Clancy, A. E., Bida, O., and Rancourt, D., Influence of advanced electromyogram (EMG) amplitude processors on EMG-to-torque estimation during constant-posture, force-varying contractions, *Journal of Biomechanics*, Vol.39 (2006), pp.2690-2698
(6) Burke, R.E., Levine, D.N., Tsairis, P., and Zajac, F.E.III, Physiological Types and Histochemical Profiles in Motor Units of the Cat Gastrocnemius, Journal of Physiology, Vol.234 (1973), pp. 723-748
(7) Bellemare, F. W., J.J., Johansson, R., and Bigland-Ritchie, B., Motor-Unit Discharge Rates in Maximal Voluntary Contractions of Three Human Muscles, *Journal of Neurophysiology*, Vol.50 (1983), pp.1380-1392.
(8) Tamura, Y., and Saito, M., A rheological motor model for vertebrate skeletal muscle in due consideration of non-linearity, *Journal of Biomechanics*, vol.35 (2002) pp.1273-1277.
(9) Tamura, Y., Saito, M., Nagato, R., A new motor model representing the stretch-induced force enhancement and shortening-induced force depression in skeletal muscle, *Journal of Biomechanics*, vol.38 (2005) pp. 877-884.
(10) Tamura, Y., Saito, M., and Ito, A., The Phenomenological Model of Muscle Contraction with a Controller to Simulate the Excitation-Contraction Coupling, *Journal of Biomechanics*, Vol. 42 (2009), pp. 400-403.
(11) Huxley, A.F., Muscle structure and theories of contraction, *Progress in Biophysics and Biophysical Chemistry,* vol.7 (1957), pp.255–318.
(12) Hatze, H., Estimation of myodynamic parameter values from observations on isometrically contracting muscle groups, *European Journal of Applied Physiology*, Vol.46 (1981), pp.325–338.
(13) Meijer, K., Grootenboer, H.J., Koopman, H.F.J.M., van der Linden, B.J.J.J., and Huijing, P.A., A Hill type model of rat medical gastrocnemius muscle that accounts for shortening history effects, *Journal of Biomechanics*, vol.31 (1998), pp.555–563.
(14) Buchthal, F., and Schmalbruch, H., Contraction Times and Fibre Types in Intact Human Muscle, *Acta Physiologica Scandinavica*, Vol.79 (1970), pp.435-452
(15) Dahmane, R., Djordjevic, S., Simunic, B., and Valencic, V., Spatial fiber type distribution in normal human muscle Histochemical and tensiomyographical evaluation, *Journal of Biomechanics*, Vol.38 (2005), pp.2451-2459